Hot-embossing fabrication of chalcogenide glasses rib waveguide for mid-infrared molecular sensing*

Ting-Yang Yan(颜庭阳)[1,2], Xiang Shen(沈祥)[1,2,†], Rong-Ping Wang(王荣平)[3], Guo-Xiang Wang(王国祥)[1,2], Shi-Xun Dai(戴世勋)[1,2], Tie-Feng Xu(徐铁峰)[1,2], and Qiu-Hua Nie(聂秋华)[1,2]

[1] *Laboratory of Infrared Material and Devices, Advanced Technology Research Institute, Ningbo University, Ningbo* 315211, *China*
[2] *Key Laboratory of Photoelectric Materials and Devices of Zhejiang Province, Ningbo* 315211, *China*
[3] *The Australian National University, Canberra, ACT* 2600, *Australia*

(Received 20 September 2016; revised manuscript received 5 December 2016; published online 10 January 2017)

Chalcogenide glasses have shown promise in fabricating mid infrared (MIR) photonic sensing devices due to their excellent optical properties in MIR. In addition, the glass transition temperature of chalcogenide glasses are generally low, making them ideal to create the high-throughput patterns of micro-scale structures based on hot embossing that is alternative to the standard lithographic technology. In this paper, we outline the research progress in the chalcogenide waveguide based on the hot embossing method, and discuss the problems remaining to be solved and the possible solutions.

Keywords: chalcogenide glasses, hot embossing, rib waveguides, MIR sensing

PACS: 42.79.Gn, 42.82.Cr, 71.23.Cq, 07.07.Df **DOI:** 10.1088/1674-1056/26/2/024213

1. Introduction

Molecular species exhibit specific vibrational absorption bands in the mid-infrared (MIR) region spanning a wavelength range from 3 μm to 25 μm.[1] Tsay *et al.*[2] indicated that MIR sensors, which are based on evanescent field sensing of molecular species, can detect the molecules at very low concentrations by using their absorption fingerprints with high sensitivity and selectivity over a wide range of compounds without labeling, and thus are potential to be applied to low-cost, widely-accessible health and environmental monitoring.[3] To detect these molecules, it is essential to develop waveguides and integrated optical devices for evanescent field based sensing in the MIR. Widely used silicate glasses do not transmit at the wavelengths beyond 3 μm, while the fluoride glasses degrade when they are in contact with water. These conventional materials that are well-characterized for the applications in the telecommunications wavelengths are not suitable for the applications in MIR. In contrast, chalcogenide glasses (ChGs), consisting of one or more chalcogen elements such as S, Se, and Te, together with other elements such as Ge, Ga, As, Si, P, and Sb,[4] are transparent in a wide range from 1 μm to 25 μm, depending on the chemical compositions,[5] covering the widely used atmospheric IR windows of 3 μm–5 μm and 8 μm–14 μm. Moreover, chalcogenide glasses are generally inert against moisture and harsh chemical surroundings, and thus are potential to be used for creating integrated devices for MIR sensing and defense applications.[6,7]

The development of chalcogenide waveguide firstly dated back to the early 1970s. Bessonov *et al.*[8] reported a chalcogenide waveguide fabricated in the form of a thin As–Se chalcogenide glass film on a barium fluoride single-crystal substrate and the attenuation coefficient measured to be 3 dB/cm for the dominant TE mode. With the further development of the fabrication techniques, Viens *et al.*[9] reported amorphous multilayer $As_{24}S_{38}Se_{38}/As_2S_3$ thin film deposited on a silicon wafer by conventional thermal evaporation and photolithography followed by chemical wet etching. Although waveguide optical loss was found to be 1 dB/cm at 1300 nm, chalcogenide waveguide structure was damaged partially (the glass sidewall etching produced ridges with a trench angle of about 45°) because most chalcogenide materials can be dissolved in alkaline resist developer NH_4OH.[10] Since the wet etching method is not easy to control, and the waveguides produced always contain particle contamination and are lack of anisotropy, more recently, plasma dry etching together with photolithography technique are usually employed to fabricate the optical waveguide. Hu *et al.*[11] reported the fabrication of the planar waveguides from thermally evaporated $Ge_{23}Sb_7S_{70}$ films by using plasma etching, the waveguide exhibits a sidewall root mean square (RMS) roughness of 17 nm–20 nm, and an optical propagation loss of 3 dB/cm–5 dB/cm at 1550 nm. To obtain better etching results, the advanced technologies like ion etching, inductively coupled plasma (ICP) technology and electron cyclotron resonance technology, have been used to fabricate chalcogenide optical waveguides. Ruan *et al.*[12] reported the fabrication of the low loss As_2S_3 rib waveguides made by standard photolithography technique combined with

*Project supported by the National Natural Science Foundation of China (Grant No. 61377061), the Public Project of Zhejiang Province, China (Grant No. 2014C31146), and sponsored by K. C. Wong Magna Fund in Ningbo University, China.

†Corresponding author. E-mail: shenxiang@nbu.edu.cn

© 2017 Chinese Physical Society and IOP Publishing Ltd

ICP, and the minimum propagation loss of the waveguide is 0.25 dB/cm at 1550 nm. Madden *et al.*[13] demonstrated that the As_2S_3 waveguides with lengths up to 22.5 cm reduce the losses down to 0.05 dB/cm at 1550 nm, which is the lowest ever reported etched by ICP.

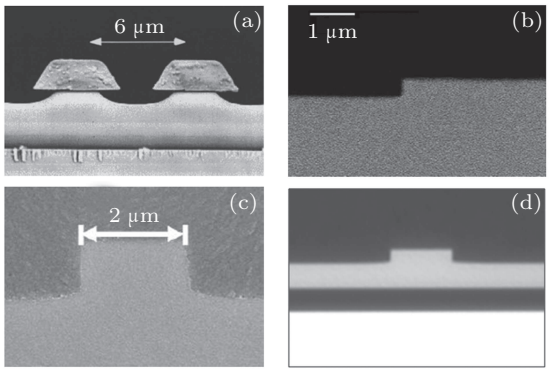


Fig. 1. (a) SEM micrograph of a multilayer $As_{24}S_{38}Se_{38}/As_2S_3$ rid waveguide processed by lithography and wet etching (Viens *et al.*).[9] (b) Cross-sectional image of $Ge_{23}Sb_7S_{70}$ waveguide patterned by SF_6 plasma etching (Hu *et al.*).[11] (c) SEM micrograph showing the profile of As_2S_3 waveguide etched by ICP and coated with polysiloxane cladding (Ruan *et al.*).[12] (d) Optical micrograph of cleaved finished waveguide in the 2.6-μm thick As_2S_3 film (Madden *et al.*).[13]

However, it is not easy to use standard photolithography followed by dry plasma etching to fabricate waveguides with high-efficiency because chalcogenides are susceptible to attack by the alkaline-based chemicals used in photolithography as well as by most gases in plasma etching. Thus some additional steps are needed, thereby leading to more complexities and less control than ideal process. All these relevant facilities require large capital investment and are not ideal for commercial large-scale production.

Hot embossing, also known as nano-imprinting, initially proposed and developed for polymeric materials by Chou *et al.*,[14,15] is an emerging lithographic technology that is based on surface patterning. It requires only a single step to fabricate complicated optical device and produce even nanometer sized features without using the chemical processing.[15–18] In contrast to standard photolithography technology, the hot embossing is extremely fast, simple and low cost, which makes it promise in large-scale production. Hot embossing is in line with the development direction of "easy" and "miniaturization" of the optoelectronic device preparation technology, hence it has received more and more attention of some well-known research institutions in recent years. In this paper, we review the fabrication of chalcogenide rib waveguide with using hot embossing and discuss further development and potential applications of this approach.

2. Hot embossing

2.1. Process of hot-embossing

Several groups have demonstrated the possibility of molding chalcogenide glasses against a stamp to make rib waveguides.[19–25] The process of hot-embossing is conceptually straightforward: chalcogenide film (deposited on silicon wafer) is heated to a temperature above its T_g (glass transition temperature), pressed against a stamp isothermally for a certain time under a prescribed load. After the removal of the load, chalcogenide film sample is cooled to ambient temperature, and then separated from the stamp manually due to tremendous differences in thermal expansion coefficient between the film and stamp material. The stamp imprint is retained in the film surface and then the desired waveguide structure is fabricated. The replication accuracy mainly depends on the quality of the surface finish of the stamp and thus it is repeatable to fabricate successive waveguides with the same stamp.[26] There are two main stamps used for hot-embossing: hard stamp and soft stamp. Hard stamp which consists of metal (e.g. Ni), silicon, fused silicon, silicon-on-insulator or metal-coated hard polymers, is usually made by e-beam lithography and wet-etching and imprinted on small areas at high loads.[27] On the other hand, soft stamp can realize multiple and diverse uniform patterning and is more tolerant to the tilt between the stamp and sample than hard stamp.[28] In addition, soft stamp is easily obtained by casting on a single master mould over large areas with excellent accuracy and reproducibility. Currently, polydimethylsiloxane (PDMS) stamp is widely used because it is sufficiently durable to permit many pattern replications and allows the production of the waveguides with no stamp release issues and good uniformity.[24,27]

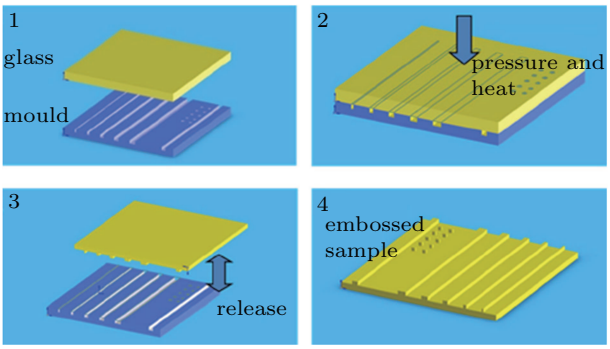


Fig. 2. (color online) Schematic flow chart of the hot embossing process. (Seddon *et al.* 2014).[26]

2.2. Core/cladding material selection

ChGs are metastable and long-range disordered materials, and compared with the crystalline material, their bonded or atomic structures tend to be more prone to change when exposed to illumination with light, thermal treatment, electromagnetic radiation and particle beam bombardment.[29] That is because (i) chalcogenide glass has a lower spatial mean coordination number (MCN), which means that it has a high degree of freedom and structural flexibility and (ii) chalcogen atoms are two-coordinated and have two high-lying lone-pair electrons on the top of its valence bands. When the chalcogenide glass is exposed to laser light, these nonbonding lone-

pair electrons are readily excited across the bandgap by the absorption of light, leading to changes in physical and optical properties of chalcogenide glass. Some distinct photoinduced phenomena are observed in amorphous chalcogenides, including photocrystallization, photovaporization, photodecomposition, photocontraction or expansion, photodarkening or photobleaching, etc. These changes are accompanied by changes in the electronic band gap, refractive index and optical absorption coefficient.[4] To summarize, ChGs exhibit distinct photosensitivity and devices such as gratings and waveguides can be fabricated in ChGs by using their photoinduced effects.[30–33] However, the excellent photosensitivity of ChGs is undesirable for fabricating waveguides via hot-embossing. Therefore, it is essential that the core material in the rib waveguide should have good photo stability and high thermal stability (i.e., it remains amorphous and does not devitrify, crystallize in the hot embossing process). Most of selenide-based glass materials have been chosen as the core glasses for fabricating waveguides via hot-embossing due to their excellent glass stability during manufacture under ambient conditions.[21–24] Generally, the waveguide is based on the chalcogenide film on an oxidized silicon wafer. For evanescent-field-mediated sensing, some groups have also employed a bulk chalcogenide glass with a lower refractive index as both the substrate and optical under-cladding (chalcogenide-on-chalcogenide).[21,22,24] To select the core and cladding glasses to make a high numerical aperture (NA) single-mode waveguide, some criteria should be meet: i) thermal expansion coefficient mismatching between the core and cladding glasses should be minimum; and ii) the cladding glass should have a higher T_g than the core glass, and this enables a range of temperatures in which the substrate is either solid or much viscous compared with the supercooled liquid thin film in this temperature range.

2.3. Film deposition

Several methods have been used to deposit high quality chalcogenide film, including thermal evaporation, radio-frequency (RF)-magnetron sputtering, ultra-fast laser ablation and collosol-gelling method. Each method has its own advantages and drawbacks, and currently thermal evaporation and radio-frequency (RF) sputtering are two main methods to deposit the films. During the thermal evaporation, the source material to be evaporated is placed in a boat and connected to a power supply for heating under vacuum conditions. When heated to a certain temperature, the solid source material is converted into gaseous particles with certain kinetic energy, leaping into high-vacuum space, and finally deposited onto the substrate surface. Thermal evaporation is convenient to prepare large-area thick film with a relatively high deposition speed, but it has problems that the deviation of component between source material and deposited film is relatively large if I) depositing materials have high melting points and II) multi-components and/or composite materials have a large melting point difference between their constituents.[34] Because non-congruent evaporation occurs, the evaporated particles with high saturated vapor pressure tend to deposit on the substrate preferentially, resulting in nonhomogeneous films. Zakery and Elliot argued that thermal evaporation might not be suitable for the accurate transfer of the stoichiometry of the multicomponent glass films.[35] Besides, the reproducibility of the film composition is not ensured and the film thickness is difficult to control precisely. On the other hand, RF sputtering is usually performed in an Argon (Ar) gas atmosphere in an evacuated chamber. When the target surface is bombarded with generated Ar^+ ions, the solid atoms emitted from the sputtered material are condensed and deposited on the surface of the substrate. Unlike thermal evaporation, RF sputtering can ensure the exact reproducibility of the film composition. However, the deposition-rate of RF-sputtering is low and the column-like structures always can be found in the deposited films, resulting in porosity.[36,37] Balan *et al.*[37] demonstrated the refractive indexes of these films were shown to decrease with increasing film thickness because of a change in the morphology (porosity) of the film.

2.4. Hard- and soft-pressing approach during the hot-embossing

There are two different approaches to hot-emboss the waveguide device: hard and soft-pressing. In the former case, the pressing facility consists of a vacuum chamber and two flat and parallel aluminum plates. The upper aluminum plate is fixed and the lower one can be raised with applied force. After the stamp is placed on the lower plate where the patterned face is up, the sample is placed on the top of the stamp where the sputtered film is faced down to the patterned stamp surface, both aluminium plates are heated to a certain temperature, and then the lower aluminium plate will be raised to accomplish the embossing [see Fig. 3(a)]. The drawback of this approach is the possible misalignment between the stamp and film and uneven loading of the film. Pan *et al.*[21] reported ChGs monomode rib waveguides fabricated by means of the hard-pressing with a hard silicon stamp in a one-step 'fiber-on-glass' approach. In the latter case, the pressing facility consists of a chamber separated by an elastic membrane. The sample with contacting the stamp sits on a hotplate and in the bottom of the chamber. The hotplate is then heated to a certain temperature, and the bottom of the chamber is evaculated and then the difference in pressure between the up and bottom of the chamber will realize the imprint isobarically [see Fig. 3(b)].[24] In this way, it is potential to be tolerant to tilt the misalignment between the stamp and sample. The pressing temperature is limited by elastic membrane, which means that

the elastic membrane should be heat resisting. Han *et al.*[24] first demonstrated a smooth-walled chalcogenide glass optical waveguide molded by soft-pressing approach with a PDMS stamp.

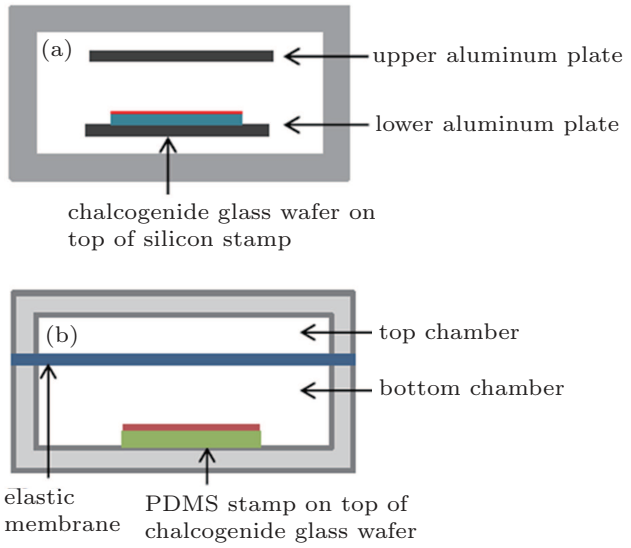


Fig. 3. (color online) Schematic diagrams of the imprinting chambers of (a) hard-pressing and (b) soft-pressing approach.

2.5. Overview of previous experiments

Pan *et al.* (2008)[21] reported a chalcogenide-glass mono-mode rib waveguide fabricated by hot-embossing through using a hard silicon stamp first in a one-step 'fiber-on-glass' approach involving two types of chalcogenide glasses (core/under-clad: $As_{40}Se_{60}/Ge_{17}As_{18}Se_{65}$). The $As_{40}Se_{60}$ fibers were hot-pressed between a silicon stamp (the fibers are aligned such that each fiber lay in one channel in the stamp) and a polished and flattened $Ge_{17}As_{18}Se_{65}$ glass substrate. One of the waveguides was an As–Se rib core with a width of 5-μm and a depth of 1.7 μm and the lowest single-mode waveguide propagation was 2.2 dB/cm for the TE mode at 1550 nm, which is in agreement with numerical modeling. The near-field image and the measured full-width-at-half-power revealed single-mode guiding [see Fig. 4]. Similar waveguides were reported by Lian *et al.* (2009)[22] who studied a hot-embossed mono-mode rib waveguide in a thermally-evaporated $As_{40}Se_{60}$ glass thin film on a $Ge_{17}As_{18}Se_{65}$ glass substrate (core: 5-μm wide and 1.9-μm high) [see Fig. 5]. Both chambers were heated to 245 °C, slightly higher than T_g of the substrate (T_g of the $Ge_{17}As_{18}Se_{65}$ glass substrate and bulk $As_{40}Se_{60}$ glass are 236 ± 2 °C and 178 ± 2 °C, respectively). At this pressing temperature, a substrate became slightly softened and enabled the rib waveguides to be evenly patterned on the thin film surface. The propagation loss was 2.9 ± 0.1 dB/cm, and this value is likely to be overestimated as the end faces of the waveguides are not ideally smooth and flat, resulting in an underestimation of the end-face reflection contribution to the measured round-trip loss.[22]

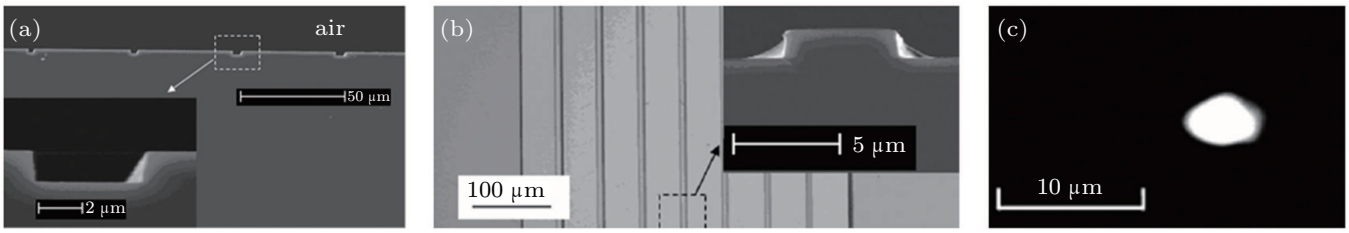


Fig. 4. SEMs of (a) Si mold cross-section and (b) top view of $As_{40}Se_{60}$ ribs on the $Ge_{17}As_{18}Se_{65}$ substrate together with a cross-sectional view at higher magnification. (c) Nearfield intensity profile observed at 1.55 μm. (Pan *et al.* 2008).[21]

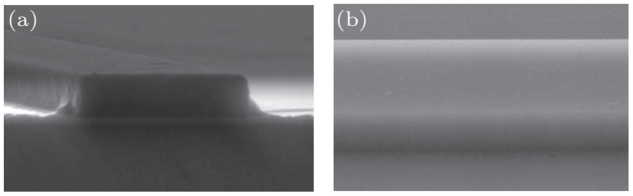


Fig. 5. SEM images of rib waveguides in the chalcogenide glass sample, showing the cross-sectional view of (a) the corresponding embossed rib waveguide and the top view (with a slight angle) of (b) the corresponding embossed glass rib waveguide. (Lian *et al.* 2009).[22]

Han *et al.* (2010)[24] reported low-loss, smooth-walled, chalcogenide glass optical waveguides molded in a single step from $As_{24}Se_{38}S_{38}$ glass film via hot-embossing with an innovative soft PDMS stamp which could produce waveguides with good surface morphology and low optical losses of 0.26 dB/cm and 0.27 dB/cm for the quasi-TM and quasi-TE polarizations, respectively, at 1550 nm (core: 2 μm–5 μm wide and 1 μm high) [see Fig. 6(a)]. However, due to the relatively low T_g of $As_{24}Se_{38}S_{38}$ glass (~110 °C) and significantly high imprint temperature (~250 °C), it was reported later (Han *et al.* 2011)[25] that severe material decomposition and crystallization occurred in the hot-embossing process, and the $As_{24}Se_{38}S_{38}$ films were found also to exhibit photosensitivity at 1550 nm. To solve these problems, the thermal evaporation of a 50-nm thick $Ge_{11.5}As_{24}Se_{64.5}$ film on the top of the thick As_2S_3 layer was used to protect the surface from degrading during embossing, and this resulted in rib waveguide with better structural stability but slightly higher optical loss of 0.52 dB/cm for the TE and 0.41 dB/cm for the TM polarizations at 1550 nm for a waveguide cross-section dimension of 3.8×1 μm [see Fig. 7] (Han *et al.* 2011).[25]

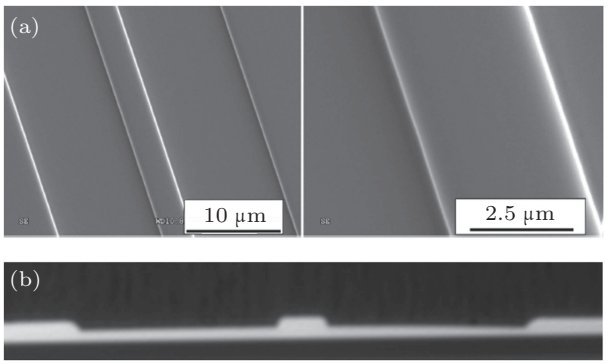


Fig. 6. SEM images of (a) imprinted rib waveguide in $As_{24}Se_{38}S_{38}$ chalcogenide glass and (b) cross sectional optical microscope view of waveguide. (Han *et al.* 2010).[24]

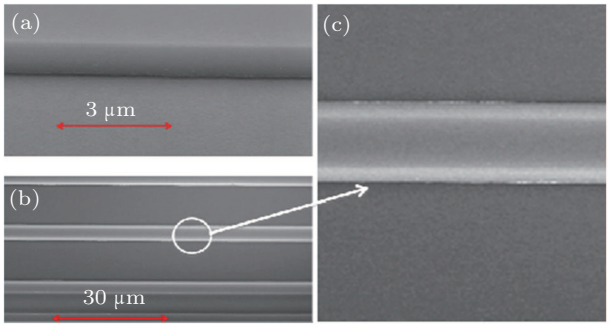


Fig. 7. (color online) SEM images of the embossed As_2S_3 waveguides: (a) side wall image at 45°; (b) plan view of the embossed waveguide surrounded by depressed trenches; (c) magnified portion from panel (b) showing some roughening at the bottom of the rib. (Han *et al.* 2011).[25]

Zou *et al.* (2013)[38] reported imprinted waveguides from thermally evaporated and solution deposited As_2Se_3 glass films by using hot-embossing. Optical loss in the waveguide fabricated from thermally evaporated film was measured to be 0.8 ± 0.3 dB/cm at 1550 nm, which is far lower than that in the waveguide from solution processed film (8.2 ± 0.6 dB/cm) by cut-back by using the optical fiber end-fire coupling. The higher loss in solution processed film is deemed to result from residual solvent absorption.[38] Abdel-Moneim *et al.* (2015)[23] reported the hot-embossing fabrication of low-loss, single-mode rib optical waveguide in RF-magnetron sputtered-deposited As_2Se_3 chalcogenide-glass thin film (core/under-clad: $As_2Se_3/Ge_{17}As_{18}Se_{65}$; core: 4 μm–6 μm wide and 1.9 ± 0.1-μm high) [see Fig. 8]. The maximum optical propagation losses measured by the Fabry–Perot technique were smaller than 0.78 dB/cm for the TE mode, and smaller than 0.81 dB/cm for the TM mode, at 1550 nm, respectively. That is because the Fabry–Perot technique is known to over-estimate the loss in most cases. It has been shown that the loss in the sputter-deposited thin film is lower than that in a thermally-evaporated $As_{40}Se_{60}$ glass thin film on a $Ge_{17}As_{18}Se_{65}$ glass substrate (Lian *et al.* 2009).[22]

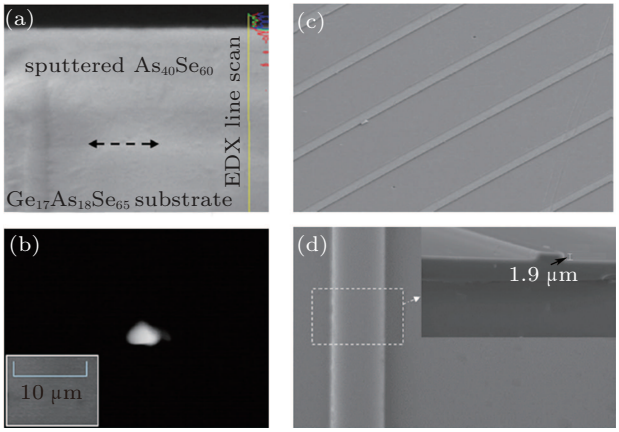


Fig. 8. (color online) For the hot-embossing waveguide from RF-sputtered As–Se thin film on the pressed Ge–As–Se substrate: (a) ESEM cross-sectional image of a cleaved edge of an RF-sputtered As–Se thin film on the top of a Ge–As–Se substrate. (b) a near-field intensity profile observed at 1550-nm wavelength in the quasi-TE mode. SEM image of (c) top view of ribs and (d) one of the ribs at higher magnification, with a cross-sectional view sown in the inset. (Abdel-Moneim *et al.* 2015).[23]

In Table 1 we list the representative hot-embossing experimental results obtained to date.

Table 1. Summary of the lowest recorded optical losses at 1550-nm wavelength for ChGs rib waveguides. The rib waveguides are shaped via hot embossing on either FOG or thermally evaporated, or RF-sputtered deposited, As–Se or As–S–Se films.

Comprising: over-clad/core/under-clad	Method of core film deposition (prior to shaping waveguides)	Lowest recorded loss of rib waveguide at 1550-nm wavelength	Ref.
Air/$As_{40}Se_{60}$/$Ge_{17}As_{18}Se_{65}$	As–Se fiber (FOG)	2.2 dB/cm for waveguides 5-μm wide × 1.7-μm deep	[21]
Air/$As_{40}Se_{60}$/$Ge_{17}As_{18}Se_{65}$	thermal evaporation	2.9 dB/cm for waveguides 5.5-μm wide × 1.9-μm deep	[22]
Air/$As_{24}S_{38}Se_{38}$/oxide-coated Si	thermal evaporation	0.26 dB/cm for quasi-TM mode, 0.27 dB/cm for quasi-TE mode, for waveguides 2- to 5-μm wide × 1-μm deep	[24]
$Ge_{11.5}As_{24}Se_{64.5}$/$As_2S_3$/ oxide-coated Si	thermal evaporation	0.52 dB/cm for the TE and 0.41 dB/cm for the TM polarizations for waveguides 3.8-μm wide × 1-μm deep	[25]
Air/As_2Se_3/oxide-coated Si	thermal evaporation	0.8 ± 0.3 dB/cm	[38]
Air/As_2Se_3/$Ge_{17}As_{18}Se_{65}$	RF-magnetron sputtering	<0.78 dB/cm for TE mode, <0.81 dB/cm for TM mode, for waveguides 4- to 6-μm wide × 1.9 ± 0.1-μm deep	[23]

3. Conclusions

Hot embossing is an emerging lithographic technology that is faster, cheaper and more scalable. Especially, hot embossing is suitable for those materials with relatively low glass transition temperature like chalcogenide glasses with T_g around 100 °C–350 °C depending on the actual chemical compositions, and thus various microstructures on the surfaces of the materials can be easily created. There are several trials to fabricate low-loss ChGs waveguides by using hot embossing processing. Han *et al.* (2010)[24] reported the first low loss ChGs waveguides fabricated by hot-embossing in $As_{24}S_{38}Se_{38}$ glass with a soft PDMS stamp. The optical loss was measured to be as low as 0.26 dB/cm at 1550 nm, which can be comparable to the best values obtained in waveguides fabricated by photolithography and dry etching. However, there are still some problems that remain to be solved: I) film decomposition, crystallization and surface evaporation or roughening may happen in the hot embossing process, and II) the sidewall structure of rib waveguide is likely to be damaged after film sample has been separated from the stamp. All these can lead to low quality waveguides. And currently, most selected film materials for hot embossing contain arsenic, which is detrimental to the environment. To overcome these problems, some solutions have been proposed: a) further selecting suitable ChGs film materials with high thermal stabilities and environment friendliness, i.e., Ge–Sb–Se system; b) coating the surface (SU-8, aluminium oxide or other ChGs film) to inhibit surface diffusion that contributes to the growth of the crystals on the surface of the core film; c) optimizing the preparation technology and trying to shorten the process of embossing at high temperature. Han *et al.*[25] have also reported that a hard h-PDMS layer is added on the surface of the softer PDMS stamp in order to increase the local rigidity and maintain global flexibility of the stamp, thereby improving the profile of the embossed waveguide.[39] In addition, it has been found that different film deposition methods have an effect on the quality of hot-embossing waveguides. For example, the optical loss of a hot-embossed rib waveguide (reported by Abdel-Moneim *et al.* 2015)[23] in an RF-magnetron sputter-deposited $As_{40}Se_{60}$ glass thin film on a $Ge_{17}As_{18}Se_{65}$ glass substrate has been demonstrated to be lower than that in a hot-embossed mono-mode rib waveguide in a thermally-evaporated $As_{40}Se_{60}$ glass thin film, on a similar $Ge_{17}As_{18}Se_{65}$ glass substrate.[22] The lower loss is believed to be due to a greater density and homogeneity of the ChGs film produced by RF-sputtering than by thermally-evaporation.[23] It is worth mentioning that the fabricating of nano-sized chalcogenide waveguides via hot embossing has not yet been reported so far, and therefore the future work on nano-size chalcogenide waveguide will be carried out to show the advantages of hot embossing technology.

References

[1] Seddon A B 2011 *Int. J. Appl. Glass Sci.* **2** 177
[2] Tsay C, Mujagić E, Madsen C K, Gmachl C F and Arnold C B 2010 *Opt. Express* **18** 15523
[3] Ródenas A, Martin G, Arezki B, Psaila N, Jose G, Jha A, Labadie L, Kern P, Kar A and Thomson R 2012 *Opt. Lett.* **37** 392
[4] Zakery A and Elliott S R 2003 *J. Non-Cryst. Solids* **330** 1
[5] Eggleton B J, Luther-Davies B and Richardson K 2011 *Nat. Photon.* **5** 141
[6] Charrier J, Brandily M L, Lhermite H, Michel K, Bureau B, Verger F and Nazabal V 2012 *Sensors and Actuators B* **173** 468
[7] Anne M L, Keirsse J, Nazabal V, Hyodo K, Inoue S, Boussard-Pledel C, Lhermite H, Charrier J, Yanakata K Loreal O, Person J L, Colas F, Compère C and Bureau B 2009 *Sensors* **9** 7398
[8] Bessonov A F, Gudzenko A I, Deryugin L N, Komotskii V A, Pogosov G A, Sotin V E and Terichev V F 1976 *Sov. J. Quantum Electron.* **6** 1248
[9] Viens J F, Meneghini C, Villeneuve A, Galstian T V, Knystautas E J, Duguay M A, Richardson K A and Cardinal T 2002 *J. Lightwave Technol.* **17** 1184
[10] Choi D Y, Madden S, Bulla D, Rode A, Wang R P and Luthe-Davies B 2011 *Phys. Status Solidi C* **8** 3183
[11] Hu J, Tarasov V, Carlie N, Petit L, Agarwal A, Richardson K and Kimerling L 2008 *Opt. Mater.* **30** 1560
[12] Ruan Y L, Li W T, Jarvis R, Madsen N, Rode A and Luther-Davies B 2004 *Opt. Express* **12** 5140
[13] Madden S J, Choi D Y, Bulla D A, Rode A V, Luther-Davies B, Ta'eed V G, Pelusi M D and Eggleton B J 2007 *Opt. Express* **15** 14414
[14] Chou S Y, Krauss P R and Renstrom P J 1995 *Appl. Phys. Lett.* **67** 3114
[15] Chou S Y, Krauss P R and Renstrom P J 1996 *J. Vac. Sci. Technol. B* **14** 4129
[16] Guo L J 2004 *J. Phys. D: Appl. Phys.* **37** R123
[17] Schift H 2008 *J. Vac. Sci. Technol. B* **26** 458
[18] Yoon K B, Choi C-G and Han S-P 2004 *Jpn. J. Appl. Phys.* **43** 3450
[19] Seddon A, Pan W, Furniss D, Miller C, Rowe H, Zhang D, McBrearty E, Zhang Y, Loni A and Sewell P 2006 *J. Non-Cryst. Solids* **352** 2515
[20] Pan W J, Furniss D, Rowe H, Miller C A, Loni A, Sewell P, Benson T M and Seddon A B 2007 *J. Non-Cryst. Solids* **353** 1302
[21] Pan W J, Rowe H, Zhang D K, Zhang Y J, Loni A, Furniss D, Sewell P, Benson T M and Seddon A B 2008 *Microw. Opt. Technol. Lett.* **50** 1961
[22] Lian Z G, Pan W J, Furniss D, Benson T M, Seddon A B, Kohoutek T, Orava J and Wagner T 2009 *Opt. Lett.* **34** 1234
[23] Abdel-Moneim N S, Mellor C J, Benson T M, Furniss D and Seddon A B 2015 *Opt. Quantum Electron.* **47** 351
[24] Han T, Madden S, Bulla D and Luther-Davies B 2010 *Opt. Express* **18** 19286
[25] Han T, Madden S, Debbarma S and Luther-Davies B 2011 *Opt. Express* **19** 25447
[26] Seddon A B, Abdel-Moneim N S, Zhang L, Pan W J, Furniss D, Mellor C J, Kohoutek T, Orava J, Wagner T and Benson T M 2014 *Opt. Eng.* **53** 71824
[27] Orava J, Kohoutek T, Greer A L and Fudouzi H 2011 *Opt. Mater. Express* **1** 796
[28] Viheriälä J, Niemi T, Kontio J, Rytkönen T and Pessa M 2007 *Electron. Lett.* **43** 150
[29] Musgraves J D, Richardson K and Jain H 2011 *Opt. Mater. Express* **1** 921
[30] Baker N J, Lee H W, Littler I C, de Sterke C M, Eggleton B J, Choi D-Y, Madden S and Luther-Davies B 2006 *Opt. Express* **14** 9451
[31] Miura K, Qiu J, Inouye H, Mitsuyu T and Hirao K 1997 *Appl. Phys. Lett.* **71** 3329
[32] Galstyan T V, Viens J F, Villeneuve A, Richardson K and Duguay M 1997 *J. Lightwave Technol.* **15** 1343
[33] Miura K, Inouye H, Qiu J, Mitsuyu T and Hirao K 1998 *Nucl. Instrum. Methods Phys. Res., Sect. B* **141** 726
[34] Seddon A B 1995 *J. Non-Cryst. Solids* **184** 44
[35] Zakery A and Elliott S R 2007 *Optical nonlinearities in chalcogenide glasses and their applications* (Berlin/Heidelberg: Springer) pp. 1–201
[36] Vigreux-Bercovici C, Labadie L, Broquin J E, Kern P and Pradel A 2005 *J. Optoelectron. Adv. Mater.* **7** 2625
[37] Balan V, Vigreux C and Pradel A 2004 *J. Optoelectron. Adv. Mater.* **6** 875
[38] Zou Y, Lin H, Li L, Danto S, Musgraves J D, Richardson K and Hu J 2013 *CLEO: Science and Innovations*, June 9–14, 2013, San Jose, California, USA, CTh1J. 5
[39] Schmid H and Michel B 2000 *Macromolecules* **33** 3042